ACS APPLIED MATERIALS & INTERFACES

Research Article

www.acsami.org

Dual Reaction-Based Multimodal Assay for Dopamine with High Sensitivity and Selectivity Using Functionalized Gold Nanoparticles

Zhanghua Zeng,* Bo Cui, Yan Wang, Changjiao Sun, Xiang Zhao, and Haixin Cui*

Institute of Environment and Sustainable Development in Agriculture, Chinese Academy of Agricultural Sciences, Beijing 100081, P.R. China

Supporting Information

ABSTRACT: A simple and dual chemical reaction-based multimodal assay for dopamine with high sensitivity and selectivity using two types of functionalized gold nanoparticles (FB-AuNPs/NsNHS-AuNPs), i.e. fluorescein modified gold nanoparticles (FB-AuNPs) and Nile blue modified gold nanoparticles (NsNHS-AuNPs), was successfully fabricated. This assay for dopamine presents colorimetric visualization and double channel fluorescence enhancement at 515 and 665 nm. The absorbance and fluorescence changes were linearly proportional to the amounts of dopamine in the range of nanomolar scale (5−100 nM). The detection limits for absorbance and fluorescence were as low as 1.2 nM and 2.9 nM (S/N = 3), respectively. Furthermore, the extent application of this multimodal assay has been successfully demonstrated in human urine samples with high reliability and applicability, showing remarkable promise in diagnostic purposes.

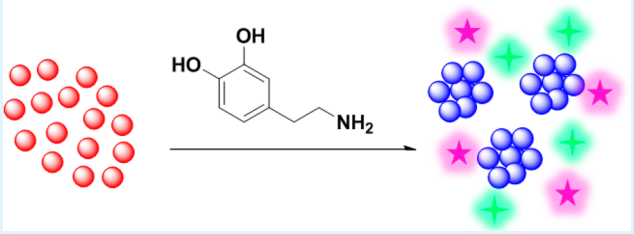

KEYWORDS: *multimodal assay, reaction-based, dopamine assay, fluorescence assay, colorimetric assay, gold nanoparticles*

INTRODUCTION

Dopamine, as one of most important hormones and neurotransmitters, plays a number of important roles in the human brain and body. Dopamine functions in motivation, motor control, reward, cognition, and arousal inside the brain.[1−4] There is clear evidence that several important central nervous system diseases are related to altered or abnormal dopamine levels, including Parkinson's disease, attention deficit hyperactivity disorder (ADHD), restless legs syndrome, and so on.[5−8] Dopamine also acts as a very important chemical messenger in several parts of the body outside the central nervous system,[9,10] and is broadly used as a biomarker to diagnose stress and pheochromocytoma in urine and plasma samples.[11,12] Given its wide-ranging physiologic and pathophysiologic effects, a highly sensitive and selective detection and determination of dopamine in biological systems is of great clinical interest and importance for medical diagnostics and for understanding its biological activities.[13] In the last few decades, several different assays in detection of dopamine based on various smart strategies have been developed, such as high performance liquid chromatography (HPLC) analysis,[14] capillary electrophoresis,[15] spectroscopic approaches,[16−18] electrochemical techniques,[19−23] surface-enhanced Raman scattering (SERS) methods,[24−26] and so on.[27−29] As dopamine is an electrochemically active molecule, electrochemical detection has extensively been developed and shows promising potential including convenience, miniaturizing, and speed. However, many coexisting compounds, such as uric acid and ascorbic acid, in real samples are electrochemically oxidized at very close potentials to that of dopamine, which greatly interferes with the accuracy and precision of measurement.[30,31] Therefore, much effort is still required to develop a really simple but highly sensitive and selective detection method of dopamine.

Recently, gold nanoparticles (AuNPs) developed as colorimetric sensors by Mirkin et al.[32,33] have been receiving a lot of attentions in the colorimetric detection of various analytes based on surface plasmon resonance (SPR) absorbance change of AuNPs without using advanced instrumentation. The SPR absorbance is highly sensitive to the interparticle distance, size, sharpness, medium, and aggregation state. Any changes in absorbance are reflected by changes in color. Thence, AuNPs have been widely used as a colorimetric assay platform for various analytes.[34−39] On the other hand, it is well-known that AuNPs very effectively quench fluorophores that are nearby, with the quenching efficiency proportional to the distance.[40,41] The quantitative fluorogenic enhancement assay could be obtained when the fluorophore slowly moved away from AuNPs in the presence of analytes.[42] Thus, these interesting and amazing features of AuNPs motivated us to explore it as a multimodal assay platform for specific bioanalytes in real urine samples.

Monomodal assay could exhibit good detection for specific analyte in simple samples. However, monomodal assay may be impotent in complex samples, as the detection channel is interfered. Multimodal assay, however, has attracted greater

Received: May 8, 2015
Accepted: July 14, 2015
Published: July 14, 2015

DOI: 10.1021/acsami.5b03956
ACS Appl. Mater. Interfaces 2015, 7, 16518−16524

attention as it can integrate two or more channels into one system to detect specific analytes.[43−45] Combining the main benefits of the colorimetric assay (quantitation and changes observable with the naked eyes) and the fluorescence assay (sensitivity and multispectral capabilities) yielded a multimodal assay with lower false-positives, better anti-interference, and greater accuracy and precision. Alone, the colorimetric or fluorescent monomodal assay could encounter heavy interference from complex samples containing chromophore or fluorophore, which then leads to lower accuracy and precision. Here, we have fabricated and demonstrated a multimodal (colorimetric and fluorogenic modalities) assay for dopamine via dual chemical reaction on the surface of functionalized AuNPs. This simple multimodal assay has been successfully applied in detection of dopamine in real urine samples with good reliability and applicability.

EXPERIMENTAL SECTION

Materials and Instruments. General reagents, chemicals, and biological samples including chloroauric acid ($HAuCl_4{\cdot}3H_2O$), trisodium citrate, dopamine, epinephrine, norepinephrine, 3,4-dihydroxyphenylacetic acid, uric acid, ascorbic acid, lactate, glucose, adenosine triphosphate, guanosine triphosphate, 5-hydroxyindoleacetic acid, homovanillic acid, thymine, bovine serum albumin, adenosine, L-tyrosine, and L-tryptophan, were purchased from Sigma-Aldrich Chemical Co., J&K Scientific, Alfa Aesar, Tokyo Chemical Industries (TCI) and Acros Organics. Unless otherwise noted, they were used without further purification. All aqueous solutions were prepared with Milli-Q water. Phosphate buffered saline solutions (PBS, pH 7.4) were obtained with 0.05 M NaH_2PO_4−Na_2HPO_4. All stock solutions of analytes were freshly prepared.

UV−vis−NIR absorbance spectra were measured on UV-2550 spectrophotometer (Shimadzu). Fluorescence experiments were carried out on RF-5301PC fluorospectrometer (Shimadzu). Absorbance and fluorescence spectra were taken after 10 min incubation. Particle size distribution and zeta-potential (ζ-potential) of dynamic light scattering (DLS) were obtained from Nano ZS90 (Malven). Transmission electron microscopy (TEM) images were taken at 200 kV using a Hitachi HF-2000. The samples of FB-AuNPs/NsNHS-AuNPs (2.0 nM) in the absence and presence of analytes were prepared at 37 °C. Fluorescence images were carried out on an Olympus inverted microscope (Olympus X71) equipped with a charge coupled device (CCD).

Synthesis of Citrate-Coated Gold Nanoparticles. Citrate-coated gold nanoparticles were obtained following the previous methods.[46] In brief, 30 mL of aqueous solution of 2.0 mM of $HAuCl_4$ hydrate was allowed to heat at reflux for 30 min, and 3.5 mL of 75 mM trisodium citrate aqueous solution was quickly added. The change in color occurred immediately from yellow, to purple, and finally wine red. The mixed reaction solution was kept boiling for 30 min, and then cooled slowly to room temperature.

Preparation of FB-AuNPs. The detailed route to preparation of FB-AuNPs was provided in Scheme S1 in the Supporting Information. For 4-mercaptophenylboronic acid-capped AuNPs, 10 mL of citrate-capped gold nanoparticles were centrifuged three times at 10 000 rpm. The pellet was collected and dispersed in PBS (pH 7.4, 50.0 mM, 10.0 mM KCl, 10.0 mM $MgCl_2$). Then, 0.1 mM 4-mercaptophenylboronic acid dispersed in 5.0 mL of PBS (containing 2% DMSO) and 0.1 mM Lip-PEG_{400} previously obtained,[46] dispersed in 5.0 mL of PBS (containing 2% DMSO), were added to 5.0 mL of citrate-capped gold nanoparticles. The mixed solution was shaken in the dark at room temperature for 6 h. The mixed solution passed through 0.4 μm sieve to remove the insoluble residue, and the filtrate was centrifuged several times at 10 000 rpm until no ligands were detected in the supernatant layer. The pellet was collected and redispersed in PBS for further synthesis.

For glucosamine-capped AuNPs, 5.0 mL of 1.0 mM D-(+)-glucosamine was added to 5.0 mL of 4-mercaptophenylboronic acid-modified AuNPs dispersed in PBS (pH 7.4, 50.0 mM). The mixed solution was shaken in the dark at room temperature for 24 h. The mixed solution passed through 0.4 μm sieve to remove the insoluble residue, and the filtrate was centrifuged several times at 10 000 rpm until no ligands were detected in the supernatant layer. The pellet was collected and redispersed in PBS for further synthesis.

To 5.0 mL of glucosamine modified AuNPs dispersed in PBS (pH 8.0) was added 5.0 mL of solution containing 2.0 mM 6-Carboxyfluorescein *N*-hydroxysuccinimide ester. The mixed solution was shaken in the dark at room temperature for 24 h. The mixed solution passed through 0.4 μm sieve to remove the insoluble residue, and the filtrate was centrifuged several times at 10 000 rpm, until no 6-carboxyfluorescein *N*-hydroxysuccinimide ester was detected in the supernatant, as verified by handy UV lamp irradiation. The obtained pellet was redispersed in PBS to afford FB-AuNPs.

Preparation of NsNHS-AuNPs. The detailed route to preparation of NsNHS-AuNPs was provided in Scheme S2 in the Supporting Information. For lipoic acid-capped AuNPs, 10 mL of citrate-capped gold nanoparticles were centrifuged three times at 10 000 rpm. The pellet was collected and dispersed in Milli-Q water, and 5.0 mL of 0.1 mM lipoic acid solution (pH 12) was added slowly within 5 min. The mixture was stirred at room temperature for 2 h. It passed through a 0.4 μm sieve to remove the insoluble residue, and the filtrate was centrifuged several times at 10 000 rpm. The pellet was collected and dispersed in PBS.

For sulfo-NHS-capped AuNPs, to the solution of lipoic acid-modified AuNPs dispersed in PBS (pH 7.4), 0.001 mol sulfo-*N*-hydroxy succinimide and 0.002 mol EDC-HCl were added in turn. The mixture was stirred at room temperature for 24 h. It passed through a 0.4 μm sieve to remove the insoluble residue, and the filtrate was centrifuged several times at 10 000 rpm. The pellet was collected and dispersed in PBS.

Two milliliters of the sulfo-NHS modified AuNPs prepared above were dispersed in PBS (pH 7.4), and Nile blue (0.001 mol) in PBS was slowly added. The mixture was stirred at room temperature for 24 h. It passed through a 0.4 μm sieve to remove the insoluble residue, and the filtrate was centrifuged several times at 10 000 rpm, until Nile blue was not detectable in supernatant. The pellet was redispersed in PBS to give NsNHS-AuNPs.

The assay for dopamine based on FB-AuNPs/NsNHS-AuNPs was obtained by simple mixing the equivalent volumes of FB-AuNPs and NsNHS-AuNPs.

Determination of Dopamine in Human Urine Samples. The fresh human urine was diluted by 100 times using PBS buffer (pH 7.4), and various amounts of dopamine were added to obtain the specific spike samples. Three samples of 24 h human urine were collected to simulate clinical test. After centrifugation at 4000 rmp twice, the supernatant of human urine samples were subjected to simple measurements using FB-AuNPs/NsNHS-AuNPs and HPLC.

RESULTS AND DICUSSION

Design Strategy and Multimodal Assay Mechanism. It is well-known that dopamine is very chemically active because of its chemical structure incorporating catechol and primary amine moieties. In principle, catechol reacts more rapidly with phenyl boronic acid than with glucose, to form stable boronic ester adduct, and the binding affinity constant is much greater (>300 times) than that of glucose under natural and weakly basic conditions.[47,48] It is very understandable that catechol has capability to instantly split the phenyl boronic ester adduct of glucose to produce more stable phenyl boronic ester adducts of catechol. On the other hand, primary amine can rapidly react with active succinimidyl ester to afford stable amide. These dual reaction-active properties enabled highly sensitive and selective multimodal assay of dopamine based on dual chemical reaction.

The multimodal assay system consists of two types of functionalized AuNPs (FB-AuNPs/NsNHS-AuNPs). FB-AuNPs were prepared with phenyl boronic ester adducts of

DOI: 10.1021/acsami.5b03956
ACS Appl. Mater. Interfaces 2015, 7, 16518−16524

Scheme 1. Schematic Illustration of Multimodal Assay for Dopamine Based on FB-AuNPs/NsNHS-AuNPs

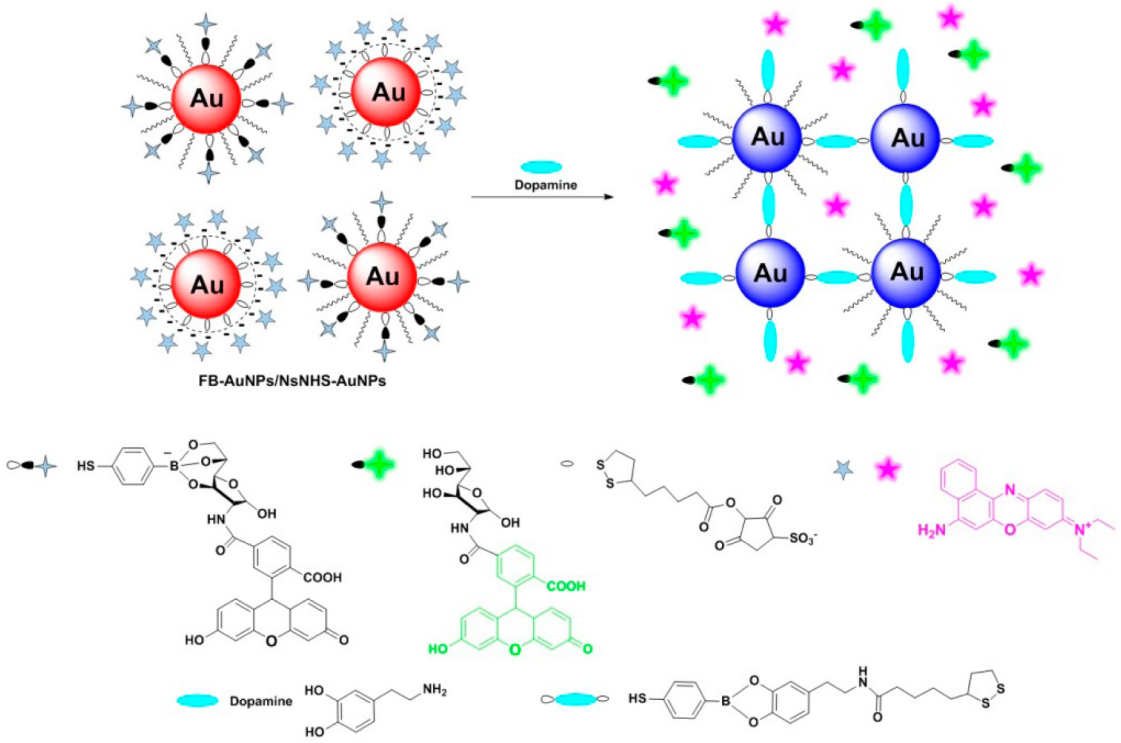

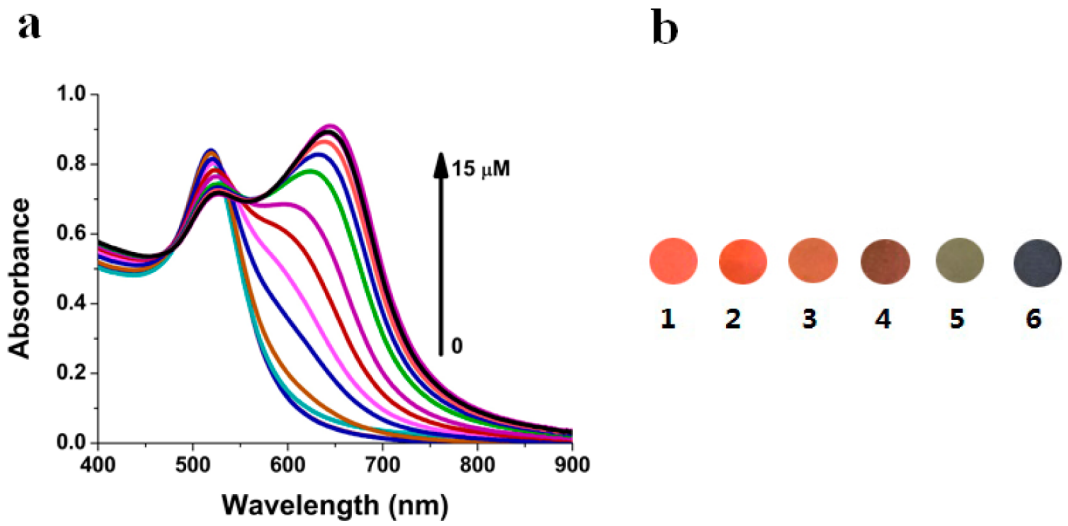

Figure 1. (a) Absorbance spectral variations of FB-AuNPs/NsNHS-AuNPs (2.0 nM) upon the addition of increasing amounts of dopamine from 0 to 15 μM. (b) Colorimetric visualization assay with different amounts of dopamine (1, 0 nM; 2, 20 nM; 3, 50 nM; 4, 100 nM; 5, 1.0 μM; 6, 15 μM). All experiments with addition of dopamine were carried out after 10 min incubation, for ensuring dual reaction completion in 50 mM PBS (pH 7.4) at 37 °C.

glucose containing a fluorescein anchoring to AuNPs, and NsNHS-AuNPs were fabricated with negatively charged sulfonated succinimidyl ester bearing a Nile blue electrostatically coated to the AuNPs. Polyethylene glycol ligand was used as coligand to stabilize FB-AuNPs in aqueous solution. The assay system was optimized with the mixture of FB-AuNPs and NsNHS-AuNPs at 1:1 ratio. In the presence of dopamine, the double reaction of boronic ester replacement and amide formation simultaneously occurred on the surface of FB-AuNPs/NsNHS-AuNPs. As a result, it induced interparticle aggregation linked by dopamine, giving rise to color change from wine red, to blue, thus allowing colorimetric visualization assay for dopamine (Scheme 1). Concomitantly, the phenyl boronic ester adducts of glucose on the surface FB-AuNPs were replaced by catechol in dopamine, and subsequently fluorescein became far away from AuNPs, resulting in fluorescence recovery of fluorescein. At the same time, the electrostatic attraction framework of NsNHS-AuNPs was destroyed, which released the Nile blue from AuNPs and recovered Nile blue fluorescence (Scheme S1 in the Supporting Information). Combining the colorimetric visualization and fluorescence

DOI: 10.1021/acsami.5b03956
ACS Appl. Mater. Interfaces 2015, 7, 16518−16524

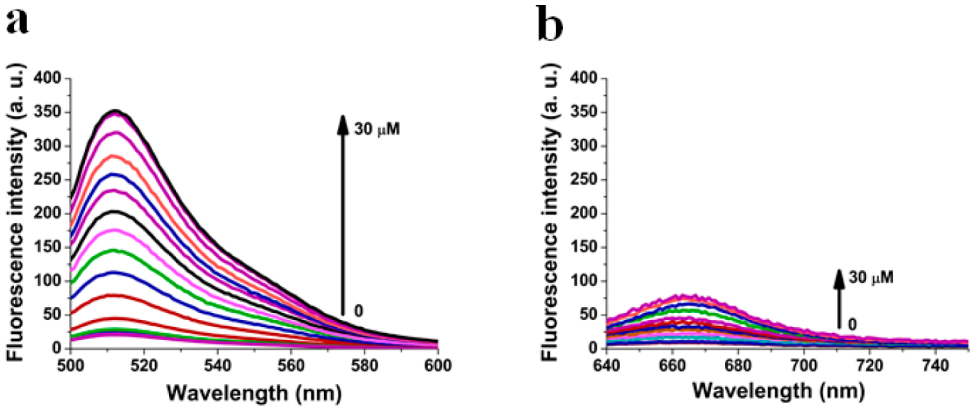

Figure 2. (a) Fluorescence spectral changes (ex: 490 nm) of FB-AuNPs/NsNHS-AuNPs (2.0 nM) upon the addition of increasing amounts of dopamine from 0 to 30 μM. (b) Fluorescence spectral changes (ex: 635 nm) of FB-AuNPs/NsNHS-AuNPs (2.0 nM) upon the addition of increasing amounts of dopamine from 0 to 30 μM. All experiments with addition of dopamine were carried out after 10 min incubation, for ensuring dual reaction completion in 50 mM PBS (pH 7.4) at 37 °C.

enhancement of fluorescein and Nile blue, the multimodal assay for dopamine was established.

Colorimetric and Fluorescent Assay for Dopamine by FB-AuNPs/NsNHS-AuNPs. To verify any changes in color when dopamine was added to FB-AuNPs/NsNHS-AuNPs, we measured the SPR absorbance of FB-AuNPs/NsNHS-AuNPs at different concentrations. FB-AuNPs, NsNHS-AuNPs and their mixture (FB-AuNPs/NsNHS-AuNPs) exhibited similarly typical absorbance peak at 522 nm, indicating negligibly small interaction of FB-AuNPs and NsNHS-AuNPs and stable mixed suspension in PBS at 37 °C. The effect of various ratios of FB-AuNPs and NsNHS-AuNPs on this assay for dopamine has been evaluated. The results showed that the optimal ratio of FB-AuNPs and NsNHS-AuNPs is 1:1 (Figure S1a, b in the Supporting Information). As expected, upon the increasing addition of dopamine, the SPR absorbance spectra presented red shift along with gradual decrease at 522 nm and an emerging peak appearance at around 644 nm (Figure 1a), suggesting that the aggregated particles were formed. In contrast, either only FB-AuNPs or only NsNHS-AuNPs showed negligible change in absorbance in the presence of dopamine (Figure S2a, b in the Supporting Information). Moreover, this assay for dopamine based on SPR absorbance spectra change was clearly visible by naked eyes from wine red to blue color, highly depending on the amounts of dopamine added (Figure 1b). These phenomena can be well-explained by the dopamine-induced aggregation of nanoparticles through double reaction-based recognition.

Because AuNPs strongly quench the fluorescence of fluorophores placed in the proximity, the fluorescence of fluorescein (covalently bonded to FB-AuNPs) and Nile blue (electrostatically attached to NsNHS-AuNPs) initially presented negligible intensity. As the binding affinity constant of phenyl boronic acid and catechol is 2 orders of magnitude greater than that of phenyl boronic acid and glucose, upon addition of dopamine, the phenyl boronic ester adduct of glucose was separated. Consequently, fluorescein was released from the surface of nanoparticles and fluorescence increased significantly by more than 16 times (Figure 2a). In the meantime, the formation of amide by the reaction of primary amine in dopamine and sulfonated succinimidyl ester on the surface of nanoparticles demolished the framework of electrostatic attraction due to loss of surface charges. Subsequently, Nile blue dissociated from the surface of nanoparticles and its fluorescence remarkably increased by nearly 18 times (Figure 2b). On the contrary, FB-AuNPs and NsNHS-AuNPs exhibited smaller changes on fluorescence at 515 and 665 nm, respectively, compared to that of FB-AuNPs/NsNHS-AuNPs (Figure S3a, b in the Supporting Information), probably due to the fact that monodispersed AuNPs are more effective quenchers than in the aggregated state.[35]

Variation of Morphology, ζ-Potential, and Size. The morphological variation of FB-AuNPs/NsNHS-AuNPs was studied by TEM. In the absence of dopamine, FB-AuNPs/NsNHS-AuNPs were fairly well monodispersed (Figure 3a).

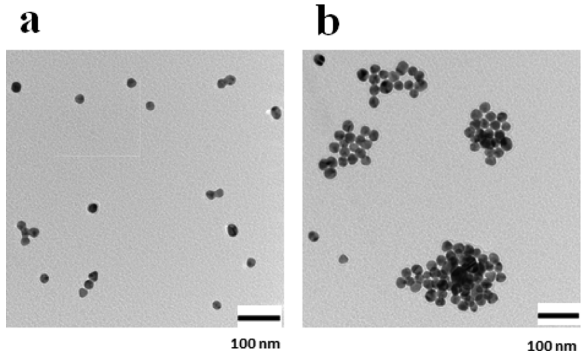

Figure 3. TEM images of FB-AuNPs/NsNHS-AuNPs (a) in the absence of dopamine and (b) in the presence of dopamine (100 nM) after 20 min incubation at 37 °C. All experiments were carried out in 50 mM PBS (pH 7.4) at 37 °C. Scale bar: 100 nm.

Upon addition of dopamine (100 nM), the internanoparticles aggregated (Figure 3b), presumably because of the formation of phenyl boronic ester adduct of catechol and amide on the surface of nanoparticles, resulting in aggregation.

DLS afforded more insight into the temporal and instant size distribution. The hydrodynamic size of FB-AuNPs/NsNHS-AuNPs gradually increased with increasing amounts of dopamine. The original size of the nanoparticles was 25 nm in PBS (pH 7.4) at 37 °C, and they grew up to 417 nm with 10 μM dopamine (Figure S4a in the Supporting Information), which is consistent with the results of the TEM observation.

This assay for dopamine based on dual reaction can be confirmed by measuring ζ-potential variation. The starting ζ-potential value of FB-AuNPs/NsNHS-AuNPs was −22.2 mV,

DOI: 10.1021/acsami.5b03956
ACS Appl. Mater. Interfaces 2015, 7, 16518−16524

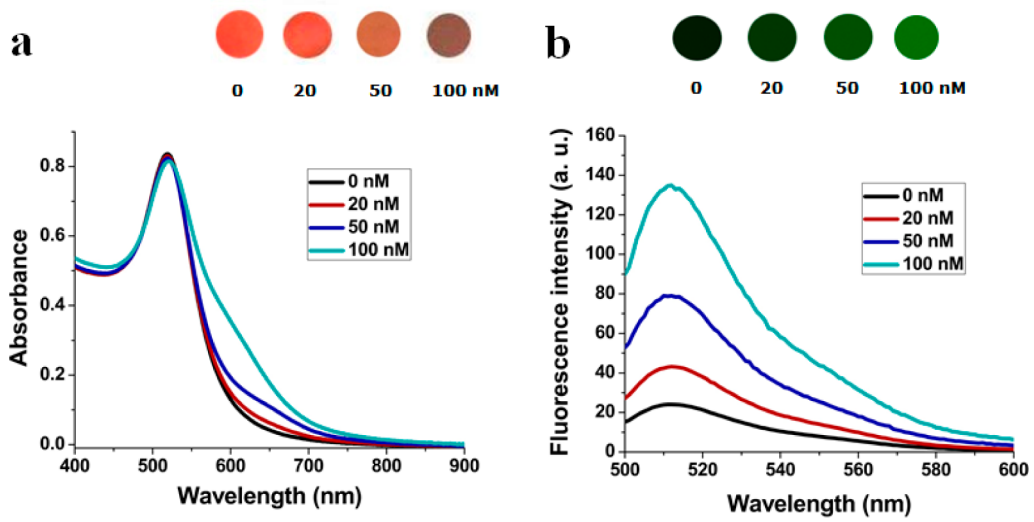

Figure 4. (a) Variation in absorbance and (b) fluorescence (ex: 490 nm) spectra of FB-AuNPs/NsNHS-AuNPs in the detection of real urine samples containing various amounts dopamine (0, 20, 50, and 100 nM). Inset: (a) colorimetric visualization and (b) fluorescence imaging assay for various amounts of dopamine (0, 20, 50, and 100 nM).

and increased gradually with increasing amounts of dopamine. It became −1.9 mV upon addition of 10 μM dopamine (Figure S4b in the Supporting Information), indicating that most of negatively charged sulfo-NHS on the surface of nanoparticles reacted with dopamine and most of fluorophores were released, agreeing well with fluorescence results.

Determination of Detection Limit. To further assess the assay performance based on FB-AuNPs/NsNHS-AuNPs, we examined an ensemble solution containing various amounts of dopamine (0, 0.005, 0.01, 0.02, 0.03, 0.06, 0.1, 0.4, 1.0, 2.0, 4.0, 8.0, 10, 12, and 15 μM). As shown in Figure 1a, the initial absorbance peak (522 nm) of FB-AuNPs/NsNHS-AuNPs decreased gradually with small red shift (525 nm), and the emerging peak at 644 nm increased at gradual manner. The ratio of absorbance value at 644 nm (A_{644}) and at 522 nm (A_{522}) versus amounts of dopamine was chosen to determine the detection limit. Plot of A_{644}/A_{522} versus the amounts of dopamine exhibited an excellent linear manner at the range of low concentration (5.0−100 nM) with good fitting correlation coefficient (R^2 = 0.99) (Figure S5a in the Supporting Information), which is much better than previous report that the addition of 175 nM dopamine was required in advance,[49] in order to overcome the low sensitivity. The detection limit for dopamine based on absorbance change of FB-AuNPs/NsNHS-AuNPs at S/N = 3 was determined as 1.2 nM. On the other hand, fitting of the ratio of fluorescence intensity (F) in the presence of various dopamine and initial fluorescence intensity (F_0) at 515 nm versus amounts of dopamine afforded similarly linear range of detection (5.0−100 nM) (Figure S5b in the Supporting Information), and 2.9 nM as detection limit value was determined at S/N = 3, in good agreement with that of absorbance change results. In theory, detection based on fluorescence yields higher sensitivity and affords better detection limit, compared with that of absorbance. In this assay, although the fluorephores were released and became away from FB-AuNPs/NsNHS-AuNPs in the presence of dopamine, the fluorescence of fluorephores was partially suppressed by AuNPs via intermolecule pathway, as AuNPs are highly effective quencher. Given that the level of dopamine is above nanomolar scale inside and outside the central nervous system, the multimodal assay in this study is practical and very applicable.

Selective Assay for Dopamine. Then, the selectivity of this analytical assay for dopamine was evaluated. The most interfering reagents in electrochemical assay, uric acid and ascorbic acid, showed very low response in color, absorbance and fluorescence. The possible coexisting interferences inside and outside of the central nervous system, including norepinephrine, epinephrine, 3,4-dihydroxyphenylacetic acid, lactate, glucose, amino acids and other biological compounds were also examined. None of them exhibited interference with colorimetric and fluorescence assay (Figures S6, S7a, S8a, and S9a in the Supporting Information), and negligible color change occurred even after 2 days. An increase in fluorescence at 665 nm was observed in the presence of some amino acids, probably due to reaction of primary amine in amino acids with sulfo-NHS on the surface of nanoparticles (Figure S9a in the Supporting Information). In addition, the effects of these interfering compounds on the specificity for dopamine assay were also investigated. Very few changes in color, absorbance, and fluorescence were observed in the combination of dopamine and above interfering compounds with specified ratio (Figures S7b, S8b, and S9b in the Supporting Information), suggesting that the selective assay for dopamine could be performed with interfering compounds.

pH Effect on the Colorimetric and Fluorescent Assay for Dopamine by FB-AuNPs/NsNHS-AuNPs. Indeed, the pH of solution highly affects dual reaction formation of phenyl boronic ester adduct and amide, thus the pH effect on this assay for dopamine was investigated in detail at 37 °C. Figure S7 in the Supporting Information revealed A_{644}/A_{522} and F/F_0 at 515 nm of FB-AuNPs/NsNHS-AuNPs with various amounts of dopamine in different pH values (from 4.0 to 9.0). Because of weak binding affinity of dopamine and phenyl boronic acid, and slow reaction rate of dopamine and sulfonated succinimidyl ester at acidic pH below 6.0, changes in the A_{644}/A_{522} and F/F_0 were very small, regardless of amounts of dopamine (Figure S7 in the Supporting Information). The fluorescence at 515 nm showed moderate intensity without analytes at acidic pH, presumably owing to a certain extent dissociation of fluorescein

DOI: 10.1021/acsami.5b03956
ACS Appl. Mater. Interfaces 2015, 7, 16518−16524

from nanoparticles. At pH above 6.8, A_{644}/A_{522} and F/F_0 at 515 and 665 nm showed remarkable responses to the amounts of dopamine, suggesting the assay is practical and applicable under physiological conditions.

Determination of Dopamine in Human Urine Samples. This simple, interesting and multimodal assay for dopamine prompted us to explore the potential application in human urine samples. First, the standard addition of dopamine to human urine samples was employed to test the applicability and reliability of this assay. As shown in Figure 4 and Table 1,

Table 1. Multimodal Determination of Dopamine in Human Spike Urine Samples Based on This Assay

urine samples	spike (nM)	found (nM)[a]	recovery (%)	RSD (n = 5, %)	found (nM)[b]	recovery (%)	RSD (n = 5, %)
1	20	19.3	96.5	4.28	19.7	98.5	4.21
2	50	51.5	103.0	2.43	49.3	98.6	2.75
3	100	99.5	99.5	2.19	98.3	98.3	2.45

[a]Data obtained based on A_{644}/A_{522}. [b]Data obtained based on F/F_0 (515 nm).

these spike urine samples can be visualized through multimodal assay based on naked eyes and fluorescence imaging. The recoveries of dopamine were determined to be 96.5, 103.0, and 99.5% based on A_{644}/A_{522} changes, and 98.5, 98.6, and 98.3% based on F/F_0 changes at 515 nm in three spike samples of dopamine, respectively. All of these relative standard deviations (RSD) were below 4.28% in five repetitions of parallel tests.

We then applied this assay to determine dopamine level in real human urine samples. Twenty-four hour urine samples were collected to simulate actual clinical tests. The results, summarized in Table 2, were comparative to conventional

Table 2. Multimodal Determination of Dopamine in Real Human Urine Samples Based on This Assay

urine samples	found (nM)[a]	found (nM)[b]	found (nM)[c]
1	93.2	91.4	86.1
2	71.1	72.5	65.7
3	82.7	84.1	76.8

[a]Data obtained based on A_{644}/A_{522}. [b]Data obtained based on F/F_0 (515 nm). [c]Data obtained based on HPLC.

methods, such as HPLC analysis, regardless of absorbance and fluorescence detection. These results confirm that this assay is applicable and reliable in detecting dopamine in real samples.

CONCLUSION

In summary, a dual molecular reaction-based colorimetric and fluorogenic assay for dopamine with high sensitivity and selectivity based on FB-AuNPs/NsNHS-AuNPs was developed. The assay relied on dual chemical reaction of replacement and amide formation on the surface of nanoparticles, giving rise to internanoparticles aggregation. The aggregation, in turn, permitted colorimetric visualization and fluorescence enhancement. The linear range of detection was obtained at nanomolar scale based on colorimetric and fluorogenic assay, and the detection limit was 1.2 nM and 2.9 nM (S/N = 3) using absorbance and fluorescence detection, respectively. This simple and multimodal assay method has been successfully demonstrated in the detection of dopamine in human urine samples with high reliability and applicability. This strategy would become promising multimodal assay platform to detect various chemical reactive molecules by introducing recognition groups on the surface of AuNPs.

ASSOCIATED CONTENT

Supporting Information

Detailed information on the prepared routes to functionalized gold nanoparticles, additional schemes and figures are provided. The Supporting Information is available free of charge on the ACS Publications website at DOI: 10.1021/acsami.5b03956.

AUTHOR INFORMATION

Corresponding Authors

*E-mail: zengzhanghua@caas.cn.
*E-mail: cuihaixin@caas.cn.

Notes

The authors declare no competing financial interest.

ACKNOWLEDGMENTS

The authors of this work are grateful to Chinese Academy of Agricultural Sciences (2015ZL042, 2060302), and National Key Basic Research Program of China (973 Program) from Ministry of Science and Technology of China (2014CB932200) for the financial support.

REFERENCES

(1) Schultz, W. Multiple Dopamine Functions at Different Time Courses. *Annu. Rev. Neurosci.* **2007**, *30*, 259−28.
(2) Björklund, A.; Dunnett, S. B. Dopamine Neuron Systems in the Brain: an Update. *Trends Neurosci.* **2007**, *30*, 194−202.
(3) Basu, S.; Dasgupta, P. S. Dopamine, a Neurotransmitter, Influences the Immune System. *J. Neuroimmunol.* **2000**, *102*, 113−124.
(4) Roitman, M. F.; Stuber, G. D.; Phillips, P. E.; Wightman, R. M.; Carelli, R. M. Dopamine Operates as a Subsecond Modulator of Food Seeking. *J. Neurosci.* **2004**, *24*, 1265−1271.
(5) Christine, C. W.; Aminoff, M. J. Clinical Differentiation of Parkinsonian Syndromes: Prognostic and Therapeutic Relevance. *Am. J. Med.* **2004**, *117*, 412−419.
(6) DeLong, M.; Wichmann, T. Changing Views of Basal Ganglia Circuits and Circuit Disorders. *Clin. EEG Neurosci.* **2010**, *41*, 61−67.
(7) Paulus, W.; Schomburg, E. D. Dopamine and the Spinal Cord in Restless Legs Syndrome: Does Spinal Cord Physiology Reveal a Basis For Augmentation? *Sleep Med. Rev.* **2006**, *10*, 185−196.
(8) Hyman, S. E.; Malenka, R. C. Addiction and the Brain: the Neurobiology of Compulsion and Its Persistence. *Nat. Rev. Neurosci.* **2001**, *2*, 695−703.
(9) Eisenhofer, G.; Kopin, I. J.; Goldstein, D. S. Catecholamine Metabolism: A Contemporary View with Implications for Physiology and Medicine. *Pharmacol. Rev.* **2004**, *56*, 331−349.
(10) Missale, C.; Nash, S. R.; Robinson, S. W.; Jaber, M.; Caron, M. G. Dopamine Receptors: from Structure to Function. *Physiol. Rev.* **1998**, *78*, 189−225.
(11) Tsunoda, M. Recent Advances in Methods for the Analysis of Catecholamines and Their Metabolites. *Anal. Bioanal. Chem.* **2006**, *386*, 506−514.
(12) Chandra, P.; Son, N. X.; Noh, H. B.; Goyal, R. N.; Shim, Y. B. Investigation on the Down Regulation of Dopamine by Acetaminophen Administration Based on Their Simultaneous Determination in Urine. *Biosens. Bioelectron.* **2013**, *39*, 139−144.
(13) Villoslada, P.; Oksenberg, J. R. Neuroinformatics in Clinical Practice: Are Computers Going to Help Neurological Patients and Their Physicians? *Future Neurol.* **2006**, *1*, 159−170.
(14) Syslova, K.; Rambousek, L.; Kuzma, M.; Najmanova, V.; Valesova, V. B.; Slamberova, R.; Kacer, P. Monitoring of Dopamine and Its Metabolites in Brain Microdialysates: Method Combining

DOI: 10.1021/acsami.5b03956
ACS Appl. Mater. Interfaces 2015, 7, 16518−16524

Freeze-drying With Liquid Chromatography−tandem Mass Spectrometry. *J. Chromatogr. A* **2011**, *1218*, 3382−3391.
(15) Park, Y. H.; Zhang, X.; Rubakhin, S. S.; Sweedler, J. V. Independent Optimization of Capillary Electrophoresis Separation and Native Fluorescence Detection Conditions for Indolamine and Catecholamine Measurements. *Anal. Chem.* **1999**, *71*, 4997−5002.
(16) Feng, J. J.; Guo, H.; Li, Y. F.; Wang, Y. H.; Chen, W. Y.; Wang, A. J. Single Molecular Functionalized Gold Nanoparticles for Hydrogen-Bonding Recognition and Colorimetric Detection of Dopamine with High Sensitivity and Selectivity. *ACS Appl. Mater. Interfaces* **2013**, *5*, 1226−1231.
(17) Feng, X. M.; Zhang, Y.; Yan, Z. Z.; Chen, N. N.; Ma, Y. W.; Liu, X. F.; Yang, X. Y.; Hou, W. H. Self-degradable Template Synthesis of Polyaniline Nanotubes and Their High Performance in the Detection of Dopamine. *J. Mater. Chem. A* **2013**, *1*, 9775−9780.
(18) Xu, Q. L.; Yoon, J. Y. Visual Detection of Dopamine and Monitoring Tyrosinase Activity Using a Pyrocatechol Violet−Sn $^{4+}$ Complex. *Chem. Commun.* **2011**, *47*, 12497−12499.
(19) Li, B.; Zhou, Y.; Wu, W.; Liu, M.; Mei, S.; Zhou, Y.; Jing, T. Highly Selective and Sensitive Determination of Dopamine by the Novel Molecularly Imprinted Poly(nicotinamide)/CuO Nanoparticles Modified Electrode. *Biosens. Bioelectron.* **2015**, *67*, 121−128.
(20) Shi, B.; Wang, Y.; Zhang, K.; Lam, T.; Chan, H. L. Monitoring of Dopamine Release in Single Cell Using Ultrasensitive ITO Microsensors Modified with Carbon Nanotubes. *Biosens. Bioelectron.* **2011**, *26*, 2917−2921.
(21) Yang, A.; Xue, Y.; Zhang, Y.; Zhang, X.; Zhao, H.; Li, X.; He, Y.; Yuan, Z. A Simple One-pot Synthesis of Graphene Nanosheet/SnO_2 Nanoparticle Hybrid Nanocomposites and Their Application for Selective and Sensitive Electrochemical Detection of Dopamine. *J. Mater. Chem. B* **2013**, *1*, 1804−1811.
(22) Zhang, L.; Cheng, Y.; Lei, J.; Liu, Y.; Hao, Q.; Ju, H. Stepwise Chemical Reaction Strategy for Highly Sensitive Electrochemiluminescent Detection of Dopamine. *Anal. Chem.* **2013**, *85*, 8001−8007.
(23) Khoobi, A.; Mehdi Ghoreishi, S.; Behpour, M.; Masoum, S. Three-Dimensional Voltammetry: A Chemometrical Analysis of Electrochemical Data for Determination of Dopamine in the Presence of Unexpected Interference by a Biosensor Based on Gold Nanoparticles. *Anal. Chem.* **2014**, *86*, 8967−8973.
(24) Tang, L.; Li, S.; Han, F.; Liu, L.; Xu, L.; Ma, W.; Kuang, H.; Li, A.; Wang, L.; Xu, C. SERS-active Au@Ag Nanorod Dimers for Ultrasensitive Dopamine Detection. *Biosens. Bioelectron.* **2015**, *71*, 7−12.
(25) An, J. H.; Choi, D. K.; Lee, K. J.; Choi, J. W. Surface-enhanced Raman Spectroscopy Detection of Dopamine by DNA Targeting Amplification Assay in Parkisons's Model. *Biosens. Bioelectron.* **2015**, *67*, 739−746.
(26) Balzerova, A.; Fargasova, A.; Markova, Z.; Ranc, V.; Zboril, R. Magnetically-Assisted Surface Enhanced Raman Spectroscopy (MA-SERS) for Label-Free Determination of Human Immunoglobulin G (IgG) in Blood Using Fe3O4@Ag Nanocomposite. *Anal. Chem.* **2014**, *86*, 11107−11114.
(27) Mao, Y.; Bao, Y.; Han, D.; Li, F.; Niu, L. Efficient One-pot Synthesis of Molecularly Imprinted Silica Nanospheres Embedded Carbon Dots for Fluorescent Dopamine Optosensing. *Biosens. Bioelectron.* **2012**, *38*, 55−60.
(28) Huang, H.; Gao, Y.; Shi, F.; Wang, G.; Shah, S. M.; Su, X. Determination of Catecholamine in Human Serum by a Fluorescent Quenching Method Based on a Water-soluble Fluorescent Conjugated Polymer−enzyme Hybrid System. *Analyst* **2012**, *137*, 1481−1486.
(29) Zhou, X.; Ma, P.; Wang, A.; Yu, C.; Qian, T.; Wu, S.; Shen, J. Dopamine Fluorescent Sensors Based on Polypyrrole/graphene Quantum Dots Core/shell Hybrids. *Biosens. Bioelectron.* **2015**, *64*, 404−410.
(30) Quan, D. P.; Tuyen, D. P.; Lam, T. D.; Tram, P. T. N.; Binh, N. H.; Viet, P. H. Electrochemically Selective Determination of Dopamine in the Presence of Ascorbic and Uric Acids on the Surface of the Modified Nafion/single Wall Carbon Nanotube/poly(3-methylthiophene) Glassy Carbon Electrodes. *Colloids Surf. B* **2011**, *88*, 764−770.
(31) Wu, D.; Li, H.; Xue, X.; Fan, H.; Xin, Q.; Wei, Q. Sensitive and Selective Determination of Dopamine by Electrochemical Sensor Based on Molecularly Imprinted Electropolymerization of o-phenylenediamine. *Anal. Methods* **2013**, *5*, 1469−1473.
(32) Mirkin, C. A.; Letsinger, R. L.; Mucic, R. C.; Storhoff, J. J. A DNA-based Method for Rationally Assembling Nanoparticles into Macroscopic Materials. *Nature* **1996**, *382*, 607−609.
(33) Elghanian, R.; Storhoff, J. J.; Mucic, R. C.; Letsinger, R. L.; Mirkin, C. A. Selective Colorimetric Detection of Polynucleotides Based on the Distance-dependent Optical Properties of Gold Nanoparticles. *Science* **1997**, *277*, 1078−1081.
(34) Liu, J.; Lu, Y. A Colorimetric Lead Biosensor Using DNAzyme-Directed Assembly of Gold Nanoparticles. *J. Am. Chem. Soc.* **2003**, *125*, 6642−6643.
(35) Saha, K.; Agasti, S. S.; Kim, C.; Li, X.; Rotello, V. M. Gold Nanoparticles in Chemical and Biological Sensing. *Chem. Rev.* **2012**, *112*, 2739−2779.
(36) Guarise, C.; Pasquato, L.; De Fillippis, V.; Scrimin, P. Gold Nanoparticles-based Protease Assay. *Proc. Natl. Acad. Sci. U. S. A.* **2006**, *103*, 3978−3982.
(37) Liu, R.; Liew, R.; Zhou, J.; Xing, B. A Simple and Specific Assay for Real-Time Colorimetric Visualization of β-Lactamase Activity by Using Gold Nanoparticles. *Angew. Chem., Int. Ed.* **2007**, *46*, 8799−8803.
(38) Jiang, T.; Liu, R.; Huang, X.; Feng, H.; Teo, W.; Xing, B. A Gold-Nanoparticel Based Colorimetric Screening Method for Baterial Enzymatic Inhibition. *Chem. Commun.* **2009**, *15*, 1972−1974.
(39) Klajn, R.; Stoddart, J. F.; Grzybowski, B. A. Nanoparticles Functionalised with Reversible Molecular and Supramolecular Switches. *Chem. Soc. Rev.* **2010**, *39*, 2203−2237.
(40) Dubertret, B.; Calame, M.; Libchaber, A. J. Single-mismatch Detection Using Gold-quenched Fluorescent Oligonucleotides. *Nat. Biotechnol.* **2001**, *19*, 365−370.
(41) Cheng, Y.; Stakenborg, T.; Van Dorpe, P.; Lagae, L.; Wang, M.; Chen, H.; Borghs, G. Fluorescence Near Gold Nanoparticles for DNA Sensing. *Anal. Chem.* **2011**, *83*, 1307−1314.
(42) Murphy, C. J.; Gole, A. M.; Stone, J. W.; Sisco, P. N.; Alkilany, A. M.; Goldsmith, E. C.; Baxter, S. C. Gold Nanoparticles in Biology: Beyond Toxicity to Cellular Imaging. *Acc. Chem. Res.* **2008**, *41*, 1721−1730.
(43) Erathodiyil, N.; Ying, J. Y. Functionalization of Inorganic Nanoparticles for Bioimaging Applications. *Acc. Chem. Res.* **2011**, *44*, 925−935.
(44) Liu, D.; Wang, Z.; Jiang, X. Gold Nanoparticles for the Colorimetric and Fluorescent Detection of Ions and Small Organic Molecules. *Nanoscale* **2011**, *3*, 1421−1433.
(45) Rana, S.; Le, N. D. B.; Mout, R.; Saha, K.; Tonga, G. Y.; Bain, R. E. S.; Miranda, O. R.; Rotello, C. M.; Rotello, V. M. A Multichannel Nanosensor for Instantaneous Readout of Cancer Drug Mechanisms. *Nat. Nanotechnol.* **2015**, *10*, 65−69.
(46) Zeng, Z.; Mizukami, S.; Kikuchi, K. Simple and Real-Time Colorimetric Assay for Glycosidases Activity Using Functionalized Gold Nanoparticles and Its Application for Inhibitor Screening. *Anal. Chem.* **2012**, *84*, 9089−9095.
(47) Yan, J.; Springsteen, G.; Deeter, S.; Wang, B. The Relationship Among pK a, pH, and Binding Constants in the Interactions Between Boronic Acids and Diols—It Is not As Simple As It Appears. *Tetrahedron* **2004**, *60*, 11205−11209.
(48) Gao, X.; Zhang, Y.; Wang, B. A Highly Fluorescent Water-soluble Boronic acid Reporter for Saccharide Sensing That Shows Ratiometric UV Changes and Significant Fluorescence Changes. *Tetrahedron* **2005**, *61*, 9111−9117.
(49) Kong, B.; Zhu, A.; Luo, Y.; Tian, Y.; Yu, Y.; Shi, G. Sensitive and Selective Colorimetric Visualization of Cerebral Dopamine Based on Double Molecular Recognition. *Angew. Chem., Int. Ed.* **2011**, *50*, 1837−1840.

DOI: 10.1021/acsami.5b03956
ACS Appl. Mater. Interfaces 2015, 7, 16518−16524